Determining Trigger Efficiency of VBF Higgs to Bottom/Charm Background Events

Zach Gillis
Fundamental Physics Directorate, SLAC National Accelerator Laboratory and Department of Physics, University of Chicago
(Dated: August 23, 2024)

The Standard Model is a well-established theory governing three fundamental interactions—strong, electromagnetic, and weak—between all known elementary particles—six quarks, six leptons, four vector bosons, and one scalar boson. The non-zero vacuum expectation value of the Higgs field is responsible for elementary particles acquiring mass, and the Higgs boson is an excitation of the Higgs field. The Higgs boson is the only spin-0 scalar boson in the Standard Model and the most recently discovered particle in the Standard Model. Studying Higgs properties—including Higgs decay modes, Higgs couplings to other elementary particles, and Higgs self-couplings—may illuminate paths to beyond Standard Model physics. This summer project assists with the VBF $H \to b\bar{b}/c\bar{c}$ event analysis within the ATLAS experiment at the Large Hadron Collider (LHC). This event—a VBF-produced Higgs decaying into either a bottom/antibottom or charm/anticharm quark pair—involves the second-largest Higgs production mode at the LHC. Within this event analysis, it is necessary to accurately account for other physics events (backgrounds) with similar detector signatures entering the analysis phase space. The primary goal of this project was to determine the trigger efficiency of the VBF event trigger for the $Z \to \mu^+\mu^-$ + jets control region (a phase space orthogonal to the signal region), which is required to yield an accurate estimate of this particular event background.

I. INTRODUCTION TO THE STANDARD MODEL

The Standard Model of particle physics is the theory that describes three of the four known fundamental interactions between all known elementary particles. It governs the electromagnetic, weak, and strong interactions but does not describe gravity. The Standard Model is based on an $SU(3) \times SU(2) \times U(1)$ gauge symmetry [1]: the $SU(3)$ symmetry describes the strong interaction between quarks and gluons as described by quantum chromodynamics (QCD), and the $SU(2) \times U(1)$ symmetry describes electroweak interactions. The Higgs mechanism is required to generate massive bosons by breaking the electroweak symmetry; therefore, the Higgs mechanism is responsible for the weak and electromagnetic interactions being separate at normal energy levels.

The Standard Model contains 17 elementary particles: six quarks, six leptons, four vector bosons, and one scalar boson. Despite its success in predicting three generations of quarks and leptons and, most recently, the Higgs boson, there are phenomena left unexplained by the Standard Model. The Standard Model does not explain the observed asymmetry between matter and antimatter in the universe (baryon asymmetry), govern gravity, incorporate any dark matter candidate particles, or explain how neutrinos acquire mass.

A. Fermions

Fermions are particles that have half-integer quantum spins and primarily form matter particles. Fermions have anti-symmetric wavefunctions; therefore, identical fermions cannot occupy the same quantum state (Pauli exclusion principle: for a two-particle system, $\Psi(x_1, x_2) = -\Psi(x_2, x_1)$; therefore, for $x = x_1 = x_2$, $\Psi(x, x) = 0$). All elementary fermions have associated antiparticles of opposite charge and have spin-1/2. The six types of quarks (called "flavors") interact with the strong force and carry one of three color charges that govern these QCD interactions. There are also six leptons: three charged leptons and three neutrinos. There are three generations of elementary fermions—each with two quarks, one charged lepton, and one neutrino. Heavier second- and third-generation fermions eventually decay via the weak interaction into lighter first-generation fermions at normal energy levels. The proton and neutron are each comprised of three first-generation quarks: the proton has two up quarks and one down quark, and the neutron has one up quark and two down quarks.

B. Bosons

Bosons are particles that have integer spins and can mediate forces. Bosons, unlike fermions, have symmetric wavefunctions; therefore, multiple identical bosons can occupy the same quantum state—a property that allows for coherent light emission from a laser or Bose-Einstein condensates. Composite bosons—formed from even numbers of fermions—are also not bound by the Pauli exclusion principle. There are five elementary bosons: four vector bosons and one scalar boson. The vector, spin-1 bosons mediate the three fundamental forces: the gluon mediates the strong force, the photon mediates the electromagnetic force, and the W^+, W^-, and Z bosons mediate the weak force. The only scalar, spin-0 boson—the

Higgs boson—is an excitation of the Higgs field.

C. Fundamental Interactions

The Standard Model includes three fundamental interactions: the electromagnetic, weak, and strong interactions.

The photon mediates the electromagnetic interaction and acts on charged particles. It is the only force felt outside the nucleus with a field strength that varies by distance.

The weak interaction—mediated by W^+, W^-, and Z bosons—allows quarks and leptons to change their flavor, typically decay to lighter particles. An example is beta-minus decay, in which a neutron decays into a proton—within the neutron, a down quark decays into a lighter up quark, mediated by a W^- boson that rapidly decays into an electron and an electron antineutrino. The weak force is unique in violating parity (P) and charge-parity (CP) symmetries. The weak force only interacts with particles with left-handed chirality or antiparticles with right-handed chirality. Evidence for CP-symmetry violation via the weak force was first found in the decay of neutral kaons (a type of meson).

Gluons mediate the strong force, which restricts quarks to hadronic particles (baryons and mesons)—this is called color confinement. Quarks and gluons both carry color charge and have interactions governed by quantum chromodynamics. Each quark can carry one of three possible colors, and each gluon can carry one of eight color combinations. The residual strong force—mediated by mesons (a composite boson)—holds together atomic nuclei.

II. INTRODUCTION TO THE HIGGS BOSON

The Higgs boson was the most recently discovered particle of the Standard Model and the only particle discovered at the Large Hadron Collider. Interactions with the Higgs field give masses to all quarks, charged leptons, and massive bosons. It is also the only spin-0 particle in the Standard Model. Therefore, studying the Higgs boson may be a path to physics beyond the Standard Model. For example, through analyzing di-Higgs production, constraints can be placed on the Higgs self-coupling constants, which provide experimental evidence for the shape of the Higgs potential. This shape informs the electroweak phase transition in the early universe—some beyond Standard Model versions of which accommodate baryon asymmetry [2]. A motivation for this analysis is probing the most prevalent Higgs decay mode—$H \to b\bar{b}$—and the so-far unobserved $H \to c\bar{c}$, which can help further constrain bottom and charm quark couplings to the Higgs field.

A. Higgs Mechanism & Electroweak Symmetry Breaking

Before the Higgs boson was discovered at the LHC in 2012, physicists theorized it as part of the Standard Model because the electroweak symmetry did not allow for massive bosons. The electroweak interaction is associated with an $SU(2) \times U(1)$ gauge symmetry. Without spontaneous symmetry breaking, there cannot be a massive gauge boson, which would violate $U(1)$ gauge invariance. Suppose that we add a mass term to the Lagrangian, $\mathcal{L}_{QED} \to \mathcal{L}_{QED} + \frac{1}{2}m^2 A^\mu A_\mu$. Under a unitary transformation $A_\mu \to A'_\mu = A_\mu - \partial_\mu \theta$. However, the mass term is not invariant under this transformation: $\frac{1}{2}m^2 A'^\mu A'_\mu = \frac{1}{2}m^2 \left(A^\mu - \partial^\mu \theta\right)\left(A_\mu - \partial_\mu \theta\right) \neq \frac{1}{2}m^2 A^\mu A_\mu$ [3]. However, gauge bosons—namely the W and Z bosons—do have mass.

Recall that the weak interaction acts only on left-handed chiral projections; thus, only the left-handed gauge transformation includes a $SU(2)_L$ transformation term. Four gauge bosons exist due to this $SU(2)_L \times U(1)_Y$ symmetry: W^1, W^2, and W^3 are associated with the $SU(2)_L$ symmetry and correspond to the weak isospin quantum number, and B is associated with the $U(1)_Y$ symmetry and corresponds to the weak hypercharge quantum number. The Higgs mechanism is required to break this electroweak symmetry, which occurs when the Higgs potential acquires a non-zero vacuum expectation value. The physical W^+ and W^- bosons in the broken symmetry are combinations of the W^1 and W^2 bosons, while the Z boson and photon are combinations of the W^3 and B bosons. The remaining symmetry is the local $U(1)$ gauge symmetry from quantum electrodynamics that allows a massless photon. Under this spontaneous symmetry breaking, only electric charge is conserved, which is the sum of the third component of weak isospin and weak hypercharge ($Q = I_3 + \frac{1}{2}Y$) [1, 4].

All elementary fermions acquire their mass via electroweak symmetry breaking through Yukawa couplings with the Higgs field. A notable exception is the neutrino—since the Standard Model does not include a neutrino with right-handed chirality, it cannot couple to the Higgs field. Another important note: most of the mass of protons and neutrons does not come from EWSB; instead, it comes from the energy stored in QCD interactions between these baryons' constituent quarks.

B. Higgs Production and Decay Modes

There are four main Higgs production modes at the LHC. The mode with the highest production cross section is gluon-gluon fusion, in which two gluons interact via a loop involving virtual heavy quarks, producing a Higgs. The second most prevalent production mode is vector boson fusion, in which massive vector bosons emitted from quarks fuse to form a Higgs—the quarks continuing to produce jets in the forward and backward regions

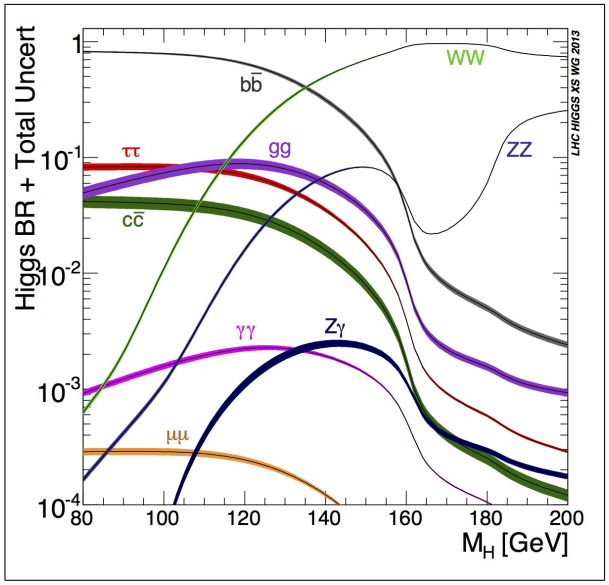

FIG. 1. Higgs branching ratio as a function of Higgs mass [5].

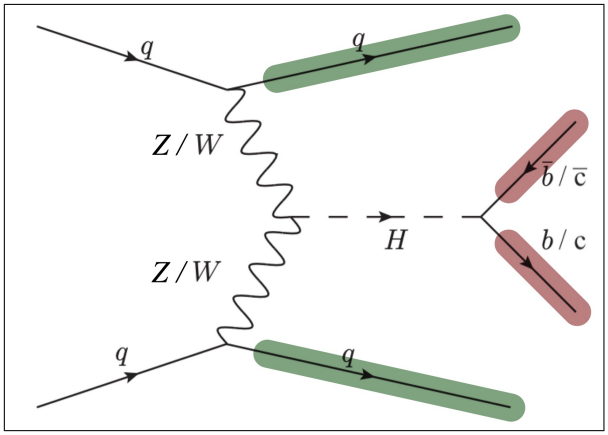

FIG. 2. Feynman diagram of VBF $H \to b\bar{b}/c\bar{c}$ event. The two high-$|\eta|$ VBF jets are shown in green, and the central bb- or cc-dijets are shown in red.

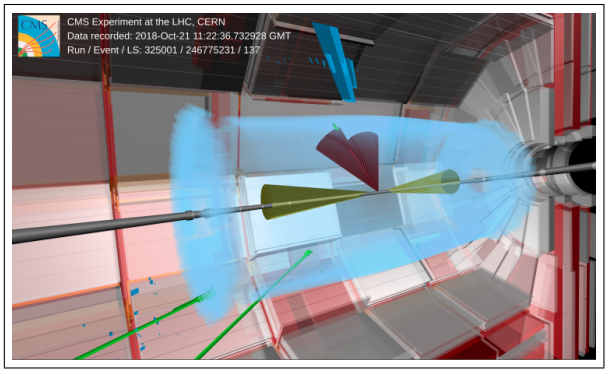

FIG. 3. Representation of VBF $H \to b\bar{b}/c\bar{c}$ detector signature. Like above, the two high-$|\eta|$ VBF jets are shown in green, and the central bb- or cc-dijets are shown in red [7].

of the detector. Other prominent production modes include vector boson and top/bottom pair associated production.

The Higgs boson has a lifetime on the order of 10^{-22} seconds; therefore, it is detected through the reconstruction of its decay products. The Higgs boson mass itself is a free parameter—one of 19 in the Standard Model—which means that it needs to be experimentally determined. The Higgs branching ratios (probabilities of each Higgs decay mode) are a function of the Higgs mass (Fig. 1). For the Standard Model Higgs, $m_H \approx 125$ GeV, $H \to b\bar{b}$ is the most likely decay mode (57%). Other prevalent decay modes are $H \to W^+W^-$, $H \to gg$, $H \to \tau^+\tau^-$, $H \to c\bar{c}$, and $H \to ZZ$.

III. VBF HIGGS TO BOTTOM/CHARM ANALYSIS

This analysis looks at vector boson fusion $H \to b\bar{b}$ and $H \to c\bar{c}$ decay events. The decay $H \to b\bar{b}$ has a high branching ratio but a significant background, while $H \to c\bar{c}$ produces c-jets that are difficult to distinguish from b-jets.

Since quarks cannot exist alone due to color confinement, they form a conical shower of hadrons called a jet within the detector. Bottom quarks travel a measurable distance through the detector before decaying (b-quarks have a lifetime of $\tau = 1.3 \cdot 10^{-12}$ s, so traveling at roughly the speed of light, $\left(1.3 \cdot 10^{-12}\text{ s}\right) \cdot c = 0.39$ mm [6]), producing a secondary vertex. Charm quarks have a shorter lifetime, so c-jets have a secondary vertex closer to the primary vertex (point of proton collision)—a distance of roughly $\left(1.1 \cdot 10^{-12}\text{ s}\right) \cdot c = 0.33$ mm [6]. Motivations for studying these two Higgs decay modes include further constraining both bottom and charm couplings to the Higgs field—deviations of these couplings from predicted values may indicate physics beyond the Standard Model. Charm quark coupling to the Higgs field is relatively poorly constrained, and VBF $H \to c\bar{c}$ has not yet been attempted in ATLAS.

Recall that vector boson fusion (Fig. 2) is the second-largest Higgs production mode in the LHC, and $H \to b\bar{b}$ is the most prevalent Higgs decay mode. The event has two distinctive VBF-jets with a high invariant mass and a high pseudorapidity gap. Since the event is electroweak in nature, there are no jets within the VBF-jet rapidity gap other than the b- and c-jets from the Higgs decay (Fig. 3).

A. What is Event Background?

Backgrounds in an event analysis are other physics events with detector signatures similar to the event of interest. They need to be subtracted from the data to yield accurate event statistics.

The primary background in this analysis is the QCD

multijet background, which is handled through data-driven methods. The background events this project focuses on are $Z \rightarrow b\bar{b}$ + jets events, which, unlike $H \rightarrow b\bar{b}$+jets, include both QCD and electroweak events. Since the Z and Higgs bosons have similar masses and b-jet energy resolution is limited, $b\bar{b}$-dijet mass distributions from Z and Higgs decays overlap significantly. Monte Carlo estimates of this background are inaccurate for this background and will be reweighed.

B. What is a Control Region?

A control region is a well-known kinematic phase space with an orthogonal output to the signal region, which is necessary to study trigger efficiency in the signal region without referencing data from the signal region.

Our signal region is the space of VBF $H \rightarrow b\bar{b}$ + jets events and backgrounds—including $Z \rightarrow b\bar{b}$+jets events. It contains events passing the VBF trigger that have at least four jets, at least one VBF-candidate jet (i.e., $p_T >$ 75 GeV, $|\eta| < 4.5$, $m_{JJ} > 1200$ GeV, $\Delta\eta_{JJ} > 4$, and $\Delta\phi_{JJ} < 2$), and two other jets that pass the b- or c-tagging requirements.

Our control region is the space of $Z \rightarrow \mu^+\mu^-$ + jets events. It similarly contains events passing the VBF trigger with at least two jets and one VBF-candidate jet, but with the Z boson decaying leptonically to two muons instead of two b-jets.

C. What is Trigger Efficiency?

Far too many events occur within the ATLAS detector than can be recorded. The two levels of the ATLAS trigger system determine which events are interesting and should be recorded. The Level-1 Trigger is a hardware trigger that processes all events with select calorimeter and muon spectrometer data and reduces the event rate from roughly 40 MHZ to 100 kHz. The High-Level Trigger is a software trigger that runs reconstruction algorithms using full detector information and reduces the event rate to 1.5 kHz [8].

The trigger efficiency of an event trigger is the proportion of events meeting the selection criteria that actually pass the trigger; studying trigger efficiency informs the parameters of the kinematic phase space in which to conduct the analysis. The trigger efficiency can depend on various kinematic variables such as jet p_T and η.

The inclusive VBF trigger aims to select events with two VBF jets, which have distinctly high invariant mass and pseudorapidity gap. To determine the VBF trigger efficiency within our control region (space of $Z \rightarrow \mu^+\mu^-$ + jets events) in a given kinematic bin, we divide the number of events that pass the VBF and loose muon triggers by the number of events that pass the loose muon trigger (the space of events passing the loose muon trigger approximates our control region). Given that trigger efficiency in data is expected to differ from that in MC, the ratio of the two trigger efficiencies in the control region is the scale factor that we will apply to the signal region MC for an accurate estimate of the signal region trigger efficiency.

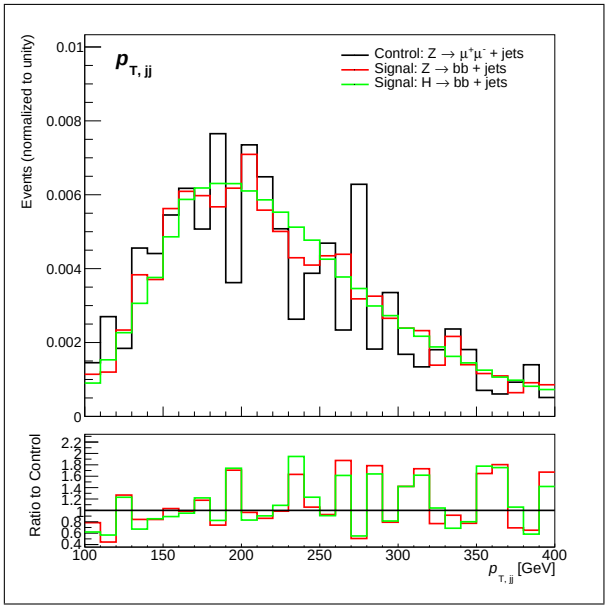

FIG. 4. High-$|\eta|$ dijet transverse momenta.

IV. CONTROL REGION VALIDATION

This section includes a series of plots that display event distributions in Monte Carlo with respect to various kinematic variables for our control and signal regions. Within our signal region, both our event ($H \rightarrow b\bar{b}$ + jets) and background of interest ($Z \rightarrow b\bar{b}$ + jets) are shown.

Figure 4 shows the dijet transverse momenta for our signal and control regions. The plot shows similar distributions in both regions, as expected.

Figure 5 shows the dijet invariant masses. The distributions of the $Z \rightarrow \mu^+\mu^-$ +jets and $Z \rightarrow b\bar{b}$+jets events have a leftward skew because they include lower mass non-VBF jets (e.g., QCD events that produce VBF-like jets).

Figure 6 shows the central dilepton and $b\bar{b}$-dijet invariant masses. The distributions of the $Z \rightarrow \mu^+\mu^-$ + jets and $Z \rightarrow b\bar{b}$ + jets events are centered around the Z boson mass of 90 GeV with a slight rightward skew. The $H \rightarrow b\bar{b}$+jets events are centered around the Higgs mass of 125 GeV with a slight leftward skew. The dilepton peaks have a better resolution than the $b\bar{b}$-dijet peaks, as the ATLAS detector reconstructs muons more precisely than jets.

Figure 7 shows the central dilepton and $b\bar{b}$-dijet invariant masses. We expected the distributions of these histograms to be roughly the same; this uncovered an issue with the event simulations that needs to be resolved.

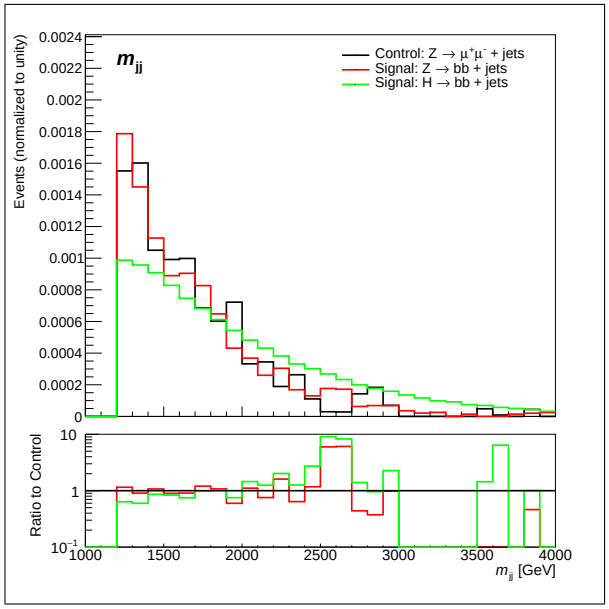

FIG. 5. High-$|\eta|$ dijet invariant masses.

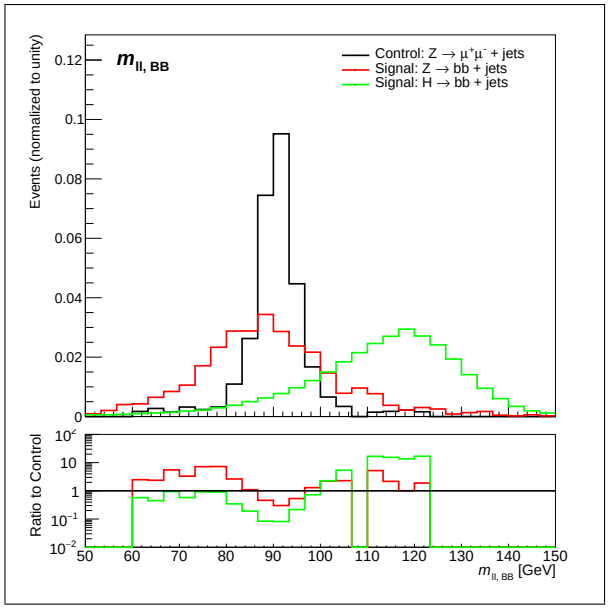

FIG. 6. Central dilepton and $b\bar{b}$-dijet invariant masses.

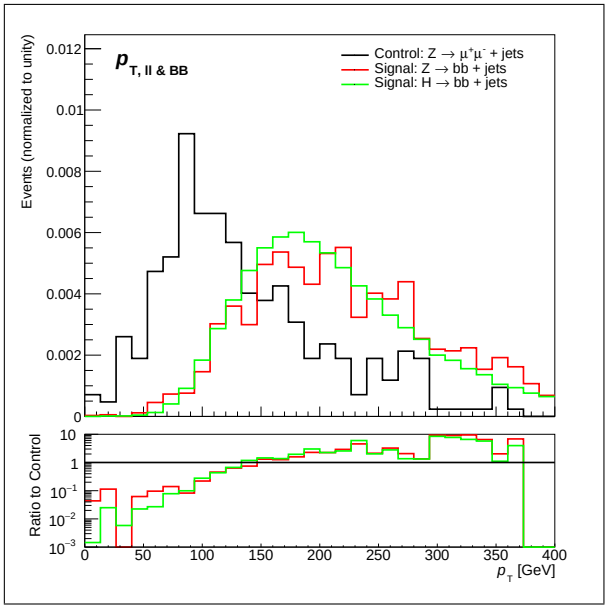

FIG. 7. Central dilepton and $b\bar{b}$-dijet transverse momenta.

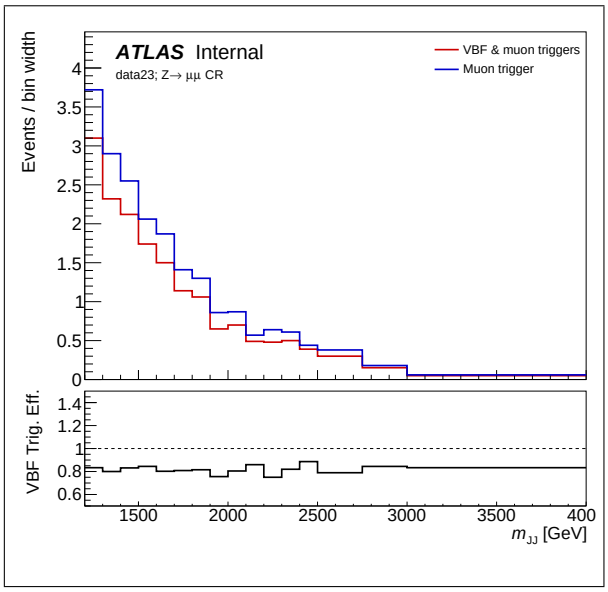

FIG. 8. Dijet mass distributions for events that pass VBF and loose muon trigger; VBF trigger efficiency in ratio panel.

V. VBF TRIGGER EFFICIENCY STUDIES

This section shows our trigger efficiencies in Monte Carlo and data for various kinematic variables in two data-taking periods. As mentioned previously, the VBF trigger efficiency within a kinematic bin of the control region is the number of events that pass the VBF and loose muon triggers divided by the number of events that pass the loose muon trigger. Figure 8 shows a the distribution for m_{JJ} in 2023 data.

Figures 9 and 10 include trigger efficiencies with respect to leading jet p_T for both periods. The ratio between data and MC trigger efficiencies is the scale factor used to reweigh the signal region MC distributions.

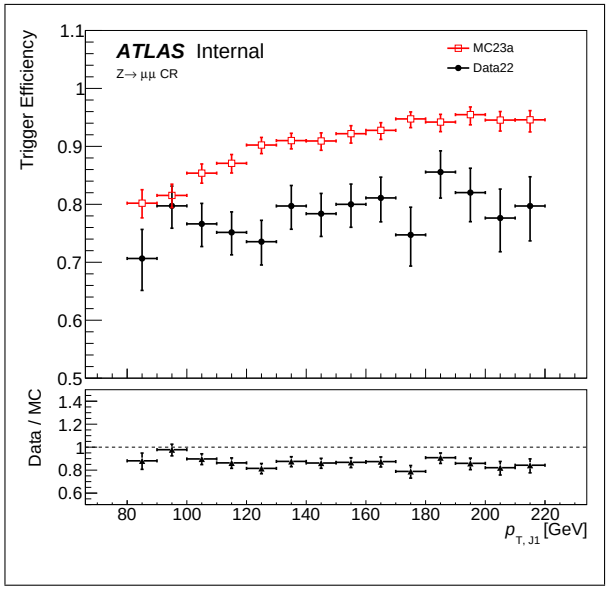

FIG. 9. Trigger efficiency with respect to $p_{T,J1}$ for MC23a/Data22.

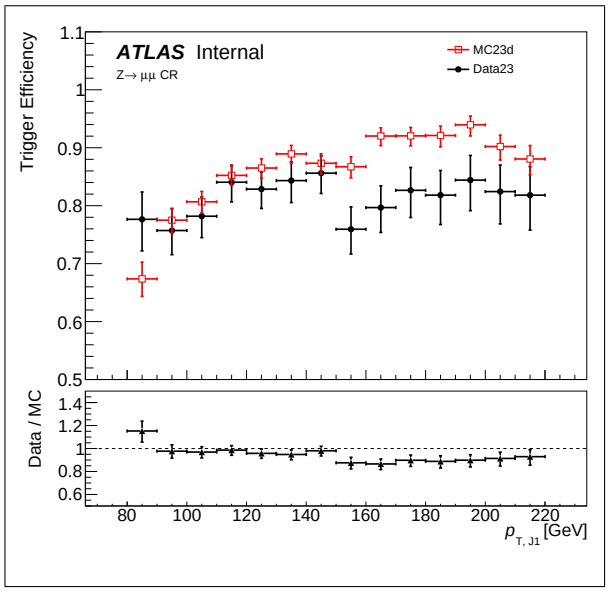

FIG. 10. Trigger efficiency with respect to $p_{T,J1}$ for MC23d/Data23.

VI. CONCLUSION

This summer project focused on analyzing vector boson fusion (VBF) Higgs boson decays into bottom and charm quark pairs within the ATLAS experiment at the Large Hadron Collider (LHC). The primary goal was to determine the trigger efficiency of the VBF event trigger within the control region of $Z \to \mu^+\mu^- +$ jets events—essential for accurately estimating the $Z \to b\bar{b} +$ jets background.

We validated the control region by examining the signal and control region Monte Carlo distributions for different kinematic variables. We also calculated the VBF trigger efficiencies in Monte Carlo and data across various kinematic variables. The ratio of the trigger efficiencies will be used to reweigh the Monte Carlo estimates in the signal region. Additionally, the control region will be used to derive transfer factors for reweighing the background events in the signal region.

ACKNOWLEDGMENTS

I want to thank the SLAC ATLAS group and SLAC National Accelerator Laboratory for making this summer opportunity possible. I especially want to thank Prajita Bhattarai and Caterina Vernieri for their support and mentorship.

This work was supported in part by the U.S. Department of Energy, Office of Science, Office of Workforce Development for Teachers and Scientists (WDTS) under the Science Undergraduate Laboratory Internships Program (SULI).

[1] A. Romanino, The standard model of particle physics, `https://www.slac.stanford.edu/econf/C0907232/pdf/001.pdf` (2009).
[2] K. Leney, Seeing double (higgs bosons) (2024), lecture notes.
[3] H. Abidi, Chronicles of the higgs boson (2024), lecture notes.
[4] K. Nguyen, The higgs mechanism, `https://www.theorie.physik.uni-muenchen.de/lsfrey/teaching/archiv/sose_09/rng/higgs_mechanism.pdf` (2009).
[5] LHC Higgs Cross Section Working Group, *Handbook of LHC Higgs Cross Sections: 3. Higgs Properties*, Tech. Rep. (CERN, 2013).
[6] J. W. Rohlf, *Modern Physics from Alpha to Z0* (John Wiley & Sons, Inc., 1994).
[7] CMS Collaboration, How does the higgs boson interact with itself? (n.d.), accessed: 2024-08-19.
[8] ATLAS Analysis Software Group, Introduction to triggers, `https://atlassoftwaredocs.web.cern.ch/AnalysisSWTutorial/trig_intro/` (2024).